

Thermodynamic Concentration Inequalities and Tradeoff Relations

Yoshihiko Hasegawa*

*Department of Information and Communication Engineering,
Graduate School of Information Science and Technology,
The University of Tokyo, Tokyo 113-8656, Japan*

Tomohiro Nishiyama

*Independent Researcher, Tokyo 206-0003, Japan
(Dated: May 1, 2024)*

Thermodynamic tradeoff relations quantify the fundamental concept of “no free lunch” in the physical world, suggesting that faster and more precise physical processes come at a higher thermodynamic cost. The key elements in these tradeoff relations are the thermodynamic uncertainty relation and speed limit, which are closely related to information inequalities from which other tradeoff relations are derived. Concentration inequalities are relations that complement information inequalities in statistical analyses and have been widely used in various fields. However, their role in thermodynamic tradeoff relations remains unclear. This study develops thermodynamic concentration inequalities that provide bounds for the distribution of observables in quantum and classical Markov processes. We derive a set of tradeoff relations that generalise speed limits and thermodynamic uncertainty relations from the developed thermodynamic concentration inequalities. The derived tradeoff relations hold under minimal assumptions of the underlying physical processes. This study clarifies the role of concentration inequalities in thermodynamics, paving the way for deriving new tradeoff relations.

The concept of tradeoff relations, illustrating the principle of no effortless gains in the physical world, has attracted considerable interest in thermodynamics. The thermodynamic uncertainty relation [1–21] (see [22] for a review) and speed limit [23–34] (see [35] for a review) are essential components of the tradeoff relations. The thermodynamic uncertainty relation implies that a thermodynamic machine requires a larger thermodynamic input to achieve a higher level of precision. The speed limit suggests that making more significant or faster changes to the state requires more thermodynamic or quantum resources.

Information inequalities, such as the Cramér-Rao inequality, are significant in statistical theory and have been widely utilised in the study of thermodynamic uncertainty relations [6, 17, 36] and speed limits [26, 33, 37]. The Cramér-Rao inequality provides the lower bound of a statistical estimator $\hat{\vartheta}$, which is given by

$$\text{Var}[\hat{\vartheta}] \geq \frac{1}{\mathcal{I}(\vartheta)}, \quad (1)$$

where ϑ is the parameter to be estimated and $\mathcal{I}(\vartheta)$ is the Fisher information. Equation (1) states that the precision of the estimator $\hat{\vartheta}$ is fundamentally limited regardless of how the estimator is constructed. Concentration inequalities constitute another pivotal class of statistical tools that, similar to information inequalities, underpin the theoretical foundation of statistical analysis [38, 39]. The most well-known instance of concentration inequality is the Markov inequality. Let X be a random variable

and let $\mathbb{E}[X]$ be the expectation of X . For a positive constant a , the Markov inequality states

$$P(|X| \geq a) \leq \frac{\mathbb{E}[|X|]}{a}. \quad (2)$$

The Markov inequality is a key concept in probability theory and statistics because of its generality; it does not necessitate knowledge of the probability distribution except for the mean. However, despite the generality and prevalence of concentration inequalities in numerous areas, including machine learning, statistics, and optimisation, they have received little attention in studying thermodynamic tradeoff relations.

This study derives the thermodynamic concentration inequalities that provide lower bounds for the probability distribution of observables in quantum and classical Markov processes. This lower bound comprises the dynamical activity, central in thermodynamic tradeoff relations [3, 5, 17, 31, 40]. From the thermodynamic concentration inequalities, we establish a family of relations that provide bounds for classical and quantum Markov processes. The derived bounds lead to generalisation of the speed limits and thermodynamic uncertainty relations (Fig. 1). The primary benefit of concentration inequalities lies in their generality. They necessitate minimal assumptions about random variables and have broad applicability, as seen in the derived thermodynamic tradeoff relations. The derivation of the thermodynamic concentration inequality opens the way to discovering new tradeoff relations in classical and quantum thermodynamics.

Open quantum dynamics

The concentration inequalities for thermodynamics can

* Corresponding author: hasegawa@biom.t.u-tokyo.ac.jp

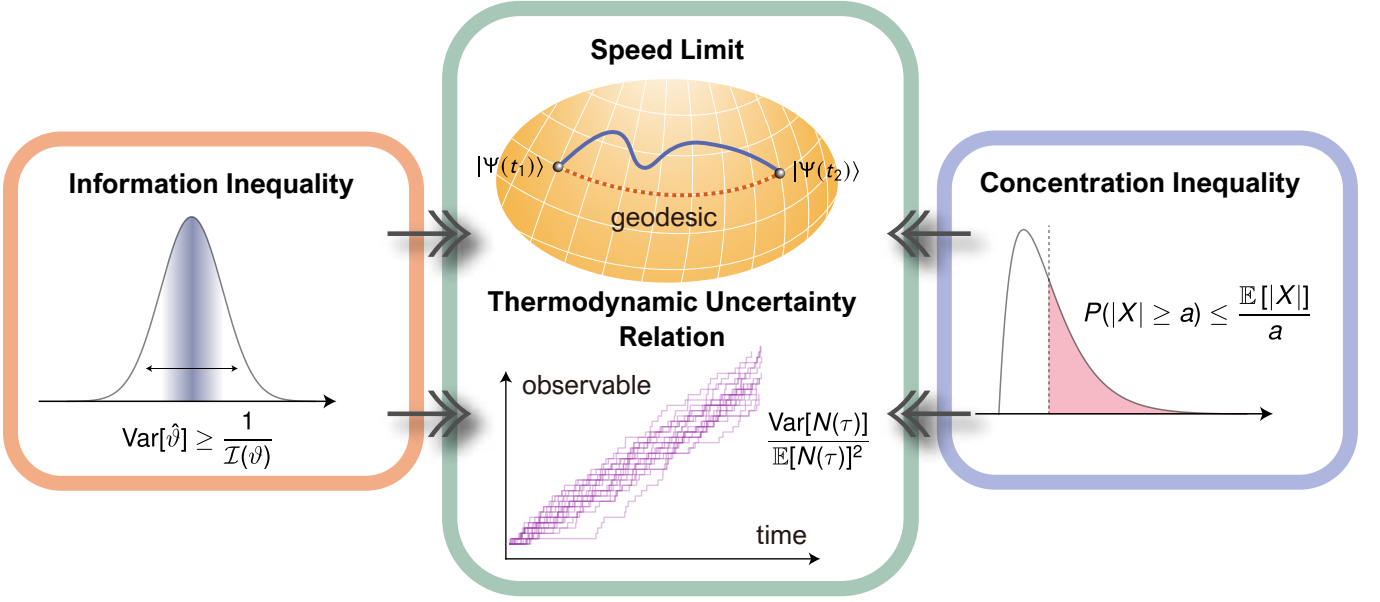


FIG. 1. **Illustrative connection between inequalities and tradeoff relations** Information inequalities, such as the Cramér-Rao inequality, are instrumental in deriving speed limits and thermodynamic uncertainty relations. This study establishes concentration inequalities as another powerful tool for establishing thermodynamic tradeoff relations.

be considered in open quantum dynamics governed by the Lindblad equation, which describes the evolution of a quantum system coupled to an external environment. Let $\rho_S(t)$ be the density operator at time t . The Lindblad equation is represented as $\dot{\rho}_S = \mathcal{L}\rho_S$, where \mathcal{L} is the Lindblad superoperator:

$$\mathcal{L}\rho_S \equiv -i[H_S, \rho_S] + \sum_{m=1}^{N_C} \mathcal{D}[L_m]\rho_S, \quad (3)$$

where H_S denotes the system Hamiltonian, L_m denotes the m th jump operator, N_C denotes the number of jump channels, and $\mathcal{D}[L]\rho_S = L\rho_S L^\dagger - \frac{1}{2}\{L^\dagger L, \rho_S\}$. The jump operators describe various dissipative processes such as energy dissipation, dephasing, and decoherence.

The Lindblad equation of Eq. (3) can describe classical Markov processes. Specifically, consider a classical Markov process comprising M states, denoted by a set $\mathfrak{B} \equiv \{B_1, B_2, \dots, B_M\}$. Let $P(\nu; t)$ be the probability that the state equals B_ν at time t and let $W_{\nu\mu}$ be the transition rate from state B_μ to state B_ν . The dynamics of the classical Markov process is described by

$$\frac{d}{dt} \mathbf{P}(t) = \mathbf{W} \mathbf{P}(t), \quad (4)$$

where $\mathbf{P}(t) \equiv [P(1; t), \dots, P(M; t)]^\top$ and the diagonal elements of $\mathbf{W} \equiv [W_{\nu\mu}]$ are defined by $W_{\mu\mu} = -\sum_{\nu \neq \mu} W_{\nu\mu}$. Then by setting $\rho_S(t) = \text{diag}[P(1; t), \dots, P(M; t)]$, $H_S = 0$, and $L_{\nu\mu} = \sqrt{W_{\nu\mu}} |B_\nu\rangle \langle B_\mu|$, where $|B_\mu\rangle$ denotes the orthogonal basis corresponding to the classical state B_μ , the Lindblad equation of Eq. (3) represents the classical dynamics of Eq. (4).

Trajectory and observable

Consider continuous measurement in the Lindblad equation corresponding to continuous monitoring of the environment coupled to the system (see the Methods section). The measurement record of the continuous measurement consists of the type of jump event and its time stamp. Suppose that the measurement record has K jump events within the interval $[0, \tau]$. The record can be expressed as

$$\zeta_\tau \equiv [(t_1, m_1), (t_2, m_2), \dots, (t_K, m_K)], \quad (5)$$

where $m_k \in \{1, \dots, N_C\}$ represents the jump type at time t_k . Here, the sequence ζ_τ is referred to as a trajectory (Fig. 2). Given the trajectory, the system dynamics can be described using a stochastic process. When averaging over all possible trajectories, the dynamics obeys the Lindblad equation of Eq. (3).

Next, we define the observables for the continuous measurement. Let $N(\zeta_\tau)$ be an observable of the trajectory ζ_τ , which is the key quantity in this study. The observable $N(\zeta_\tau)$ can be arbitrary as long as the following condition is satisfied:

$$N(\zeta_\emptyset) = 0, \quad (6)$$

where ζ_\emptyset denotes the trajectory with no jumps. In the following, we simplify the notation $N(\zeta_\tau)$ to $N(\tau)$. An example of $N(\tau)$ that satisfies Eq. (6) is the counting observable:

$$N(\tau) = \sum_m C_m N_m(\tau), \quad (7)$$

where $[C_m]$ is the real weight vector and N_m is the number of m th jump within $[0, \tau]$. For example, the thermodynamic uncertainty relation in Ref. [3] concerns the

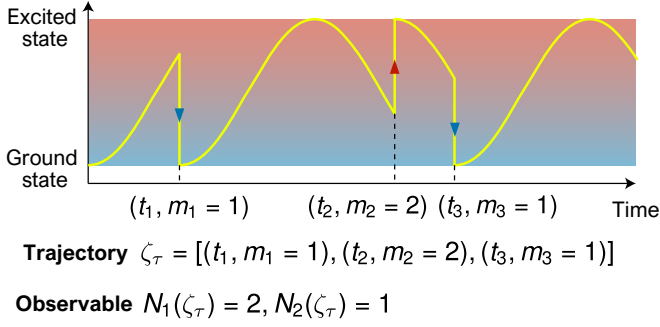


FIG. 2. **Continuous measurement and trajectory.** Two-level system comprising the excited state $|\epsilon\rangle$ and ground state $|\mathbf{g}\rangle$. The Hamiltonian is $H_S \propto |\epsilon\rangle\langle\mathbf{g}| + |\mathbf{g}\rangle\langle\epsilon|$ and two jump operators are $L_1 \propto |\mathbf{g}\rangle\langle\epsilon|$ and $L_2 \propto |\epsilon\rangle\langle\mathbf{g}|$. During the continuous measurement, the Hamiltonian H_S generates smooth dynamics, while the jump operators L_1 and L_2 cause transitions to the ground and excited states, respectively. The occurrence of jump types $m = 1, 2$, and 1 are at $t = t_1, t_2$, and t_3 in that order. The observable $N_m(\tau)$, which counts the number of jumps within $[0, \tau]$, is $N_1(\tau) = 2$ and $N_2(\tau) = 1$.

counting observable in Eq. (7). Since ζ_τ is a random variable, $N(\tau)$ is also a random variable. Therefore, we can consider its probability distribution $P(N(\tau))$, which plays a central role in this study.

Thermodynamic cost

Here, we introduce the relevant thermodynamic quantities. We first review classical dynamical activity, a central cost term in thermodynamic tradeoff relations [3, 5, 31]. The classical dynamical activity was originally proposed as an order parameter in the field of glass transitions [41]. In classical Markov processes, the time-integrated dynamical activity within $[0, \tau]$ is defined as $\mathcal{A}_{\text{cl}}(\tau) \equiv \int_0^\tau \mathbf{a}(t) dt$, where $\mathbf{a}(t)$ is the dynamical activity at t :

$$\mathbf{a}(t) \equiv \sum_{\nu, \mu (\nu \neq \mu)} P(\mu; t) W_{\nu\mu}. \quad (8)$$

$\mathcal{A}_{\text{cl}}(t)$ evaluates the average number of jump events within $[0, \tau]$ and thus it quantifies the activity of the system. Using the jump operator L_m , classical dynamical activity can be represented by

$$\mathcal{A}(\tau) \equiv \int_0^\tau \sum_m \text{Tr}_S [L_m \rho_S(t) L_m^\dagger] dt, \quad (9)$$

where Tr_S is the trace with respect to the system. The equivalence between $\mathcal{A}_{\text{cl}}(\tau)$ and $\mathcal{A}(\tau)$ for the classical limit is confirmed by assigning $L_m = L_{\nu\mu} = \sqrt{W_{\nu\mu}} |B_\nu\rangle\langle B_\mu|$ in Eq. (9), and considering the density operator $\rho_S(t)$ whose diagonal entries follow the probability distribution $P(\mu; t)$.

The concept of dynamical activity can be generalised to the open quantum dynamics described by the Lindblad equation, which plays a central role in tradeoff relations

[17, 40, 42–44]. Let $\mathcal{B}(\tau)$ be the quantum generalisation of $\mathcal{A}(\tau)$ in Eq. (9), called the quantum dynamical activity. Because the classical dynamical activity measures the level of system activity determined by jump statistics, $\mathcal{B}(\tau)$ evaluates the activity of open quantum dynamics within $[0, \tau]$. In quantum dynamics, state changes can occur even without a jump, owing to the coherent dynamics. Thus, $\mathcal{B}(t)$ includes contributions from jump and coherent dynamics. As mentioned, the classical case can be covered by considering specific H_S and L_m in the Lindblad equation [Eq. (3)] in which $\mathcal{B}(t)$ reduces to $\mathcal{A}(t)$ for the classical case. Details on the quantum dynamical activity are presented in the Methods section.

Thermodynamic concentration inequality

Because the dynamical activities in classical and quantum models measure the degree of activity, these measures could have a quantitative relationship with the probability distribution $P(N(\tau))$. We claim that the dynamical activity and probability $P(N(\tau) = 0)$ are related by inequalities. Specifically, for $0 \leq (1/2) \int_0^\tau \sqrt{\mathcal{B}(t)}/t dt \leq \pi/2$, the thermodynamic concentration inequality holds:

$$\cos \left[\frac{1}{2} \int_0^\tau \frac{\sqrt{\mathcal{B}(t)}}{t} dt \right]^2 \leq P(N(\tau) = 0). \quad (10)$$

Equation (10) is the key component for obtaining trade-off relations through other concentration inequalities. A proof of Eq. (10) is presented in the Methods section. As the quantum dynamical activity, denoted by $\mathcal{B}(t)$, increases, the probability $P(N(\tau) = 0)$ decreases. Consequently, the left-hand side of Eq. (10) decreases, which aligns with our intuitive understanding. Equation (10) can be equivalently expressed using $\sin \left[(1/2) \int_0^\tau \sqrt{\mathcal{B}(t)}/t dt \right]^2 \geq P(|N(\tau)| > 0)$, which estimates the probability that $|N(\tau)|$ deviates from 0. In the classical limit, $\mathcal{B}(\tau)$ is simplified to $\mathcal{A}(\tau)$ to directly derive the classical case of Eq. (10). For a time-independent classical Markov process and $0 \leq (1/2) \int_0^\tau \sqrt{\mathcal{A}(t)}/t dt \leq \pi/2$, we obtain

$$\cos \left[\frac{1}{2} \int_0^\tau \frac{\sqrt{\mathcal{A}(t)}}{t} dt \right]^2 \leq P(N(\tau) = 0). \quad (11)$$

Any relations that hold for $\mathcal{B}(\tau)$ should hold for $\mathcal{A}(\tau)$ when considering the classical limit. For classical Markov processes, a different concentration inequality holds. For a time-independent classical Markov process, we obtain

$$e^{-\mathbf{a}(0)\tau} \leq P(N(\tau) = 0), \quad (12)$$

where $\mathbf{a}(t)$ denotes the rate of dynamical activity [Eq. (8)]. A proof of Eq. (12) is presented in the Methods section. A notable advantage of Eq. (12) over Eq. (11) is that it holds for any $\tau > 0$. In general, it is unknown which of Eqs. (11) and (12) is tighter. However, in the steady-state condition, Eq. (12) is tighter.

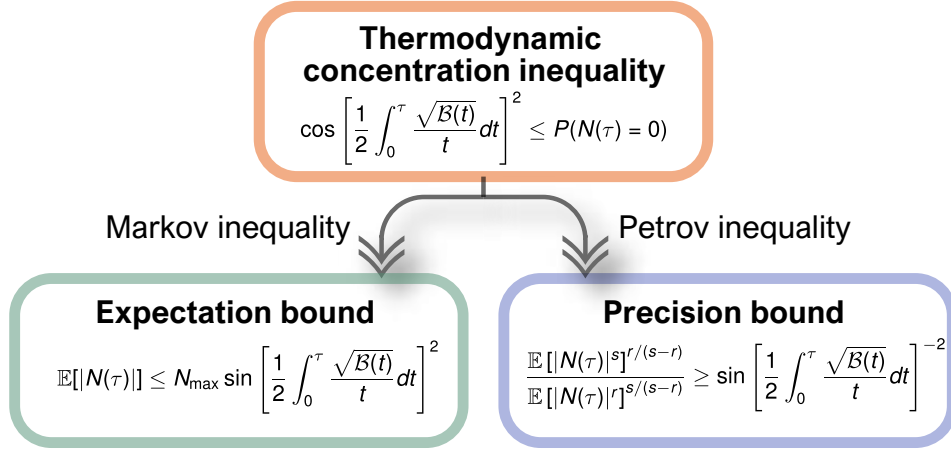


FIG. 3. **Illustration of the relationship between obtained inequalities.** The central inequality for quantum Markov processes is the thermodynamic concentration inequality [Eq. (10)]. By combining it with other concentration inequalities, other tradeoff relations can be derived. For example, combining it with the Markov inequality [Eq. (2)] and the Petrov inequality [Eq. (20)] yield the expectation bound [Eq. (13)] and precision bound [Eq. (21)], respectively. Similar relations are established from Eq. (12) for classical Markov processes. Furthermore, tradeoff relations such as speed limits can be derived from the expectation and precision bounds.

Expectation bound

In the previous section, we derived concentration inequalities in the context of classical and quantum thermodynamics. The obtained concentration inequalities provide bounds on the number of jumps and assist in deriving various tradeoff relations. We obtain tradeoff relations that can be derived from Eqs. (10)–(12) by combining them with the other concentration inequalities. The most well-known concentration inequality is the Markov inequality [Eq. (2)], considered a fundamental tool because of its simplicity and generality. It does not require knowledge of the probability distribution, only its mean. Using the Markov inequality, we can derive an upper bound for $\mathbb{E}[|N(\tau)|]$. Let N_{\max} be the maximum of $|N(\tau)|$. Then, for $0 \leq (1/2) \int_0^\tau \sqrt{B(t)}/t dt \leq \pi/2$, the following relation can be derived from Eq. (10):

$$\mathbb{E}[|N(\tau)|] \leq N_{\max} \sin \left[\frac{1}{2} \int_0^\tau \frac{\sqrt{B(t)}}{t} dt \right]^2. \quad (13)$$

For a classical Markov process, the following relation can be derived from Eq. (12):

$$\mathbb{E}[|N(\tau)|] \leq N_{\max} (1 - e^{-a(0)\tau}). \quad (14)$$

Proofs of Eqs. (13) and (14) are based on the application of Eqs. (10) and (12) to the Markov inequality, as shown in the Methods section. Given the general observables satisfying Eq. (6), Eqs. (13) and (14) hold for any quantum and classical Markov processes, respectively. Equation (13) is similar to the bounds derived in Ref. [45]. Indeed, we can derive inequalities that provide upper bounds to the correlation function, as in Ref. [45]. Moreover, from the correlation inequalities, we can obtain an upper bound for the response against perturbation in a

classical Markov process using the linear response theory. This is discussed in detail in the Methods section.

Probability theory and statistics use the integral probability metric to measure the distance between two probability distributions. It includes several well-known distance metrics, such as the Wasserstein-1 distance and the total variation distance. Speed limits in classical Markov processes can be derived using the integral probability metric using Eq. (14). Classical speed limits using the integral probability metric were recently considered in Ref. [46], which proposed deriving several uncertainty relations in a unified framework. The integral probability metric between two probability distributions $\mathfrak{P}(X)$ and $\Omega(Y)$ is defined as follows:

$$D_{\mathcal{F}}(\mathfrak{P}, \Omega) \equiv \max_{f \in \mathcal{F}} |\mathbb{E}_{\mathfrak{P}}[f(X)] - \mathbb{E}_{\Omega}[f(Y)]|, \quad (15)$$

where $\mathbb{E}_{\mathfrak{P}}[\bullet]$ denotes the expectation with respect to $\mathfrak{P}(X)$. Here, \mathcal{F} denotes a class of real-valued functions and their choice specifies the type of distance. For example, Eq. (15) expresses the total variation distance, where \mathcal{F} is a set of indicator functions that return either 0 or 1. We consider the following observable $N(\tau)$:

$$N(\tau) = f(X(\tau)) - f(X(0)). \quad (16)$$

Subsequently, the expectation is

$$\mathbb{E}[N(\tau)] = \mathbb{E}_{\mathbf{P}(\tau)}[f(X(\tau))] - \mathbb{E}_{\mathbf{P}(0)}[f(X(0))]. \quad (17)$$

From Eq. (17), $D_{\mathcal{F}}(\mathbf{P}(0), \mathbf{P}(\tau)) = \max_{f \in \mathcal{F}} \mathbb{E}[N(\tau)]$. Substituting Eq. (17) into Eq. (14), the following result is obtained:

$$D_{\mathcal{F}}(\mathbf{P}(\tau), \mathbf{P}(0)) \leq F_{\max} (1 - e^{-a(0)\tau}), \quad (18)$$

where

$$F_{\max} \equiv \max_{X_1, X_2 \in \mathfrak{B}} |f_{\max}(X_1) - f_{\max}(X_2)|, \quad (19)$$

where $f_{\max} \equiv \arg\max_{f \in \mathcal{F}} \mathbb{E}[N(\tau)]$. As mentioned, depending on the choice of \mathcal{F} , Eq. (18) becomes a bound for a different distance function. We discuss only the speed limits of classical Markov processes. However, their quantum generalisation is not trivial because the quantum distance measure does not permit an integral probability metric representation.

Precision bound

Next, we relate the probability $P(N(\tau) = 0)$ to the norm of $N(\tau)$ using another concentration inequality, namely Petrov inequality (Eq. (9) in [47]):

$$P(|X| > b) \geq \frac{(\mathbb{E}[|X|^r] - b^r)^{s/(s-r)}}{\mathbb{E}[|X|^s]^{r/(s-r)}}, \quad (20)$$

where $0 < r < s$, $b \geq 0$, and the condition $b^r \leq \mathbb{E}[|X|^r]$ should be satisfied. The well-known Paley-Zygmund inequality [48] can be obtained by substituting $r = 1$, $s = 2$, and $b = \lambda \mathbb{E}[|X|]$ in Eq. (20), where $0 \leq \lambda \leq 1$. Using Eqs. (10), (12), and (20), the thermodynamic uncertainty relation can be generalised. For $0 \leq (1/2) \int_0^\tau \sqrt{\mathcal{B}(t)}/t dt \leq \pi/2$ and $0 < r < s$, the following relation holds:

$$\frac{\mathbb{E}[|N(\tau)|^s]^{r/(s-r)}}{\mathbb{E}[|N(\tau)|^r]^{s/(s-r)}} \geq \sin \left[\frac{1}{2} \int_0^\tau \frac{\sqrt{\mathcal{B}(t)}}{t} dt \right]^{-2}. \quad (21)$$

Moreover, for the classical Markov process, we obtain

$$\frac{\mathbb{E}[|N(\tau)|^s]^{r/(s-r)}}{\mathbb{E}[|N(\tau)|^r]^{s/(s-r)}} \geq \frac{1}{1 - e^{-\mathbf{a}(0)\tau}}. \quad (22)$$

A proof of Eqs. (21) and (22) is a direct application of Eqs. (10) and (12) to Eq. (20) (see the Methods section). Equations (21) and (22) hold for arbitrary time-independent quantum and classical Markov processes with arbitrary initial states, respectively. For the random variable X , we define the p -norm as $\|X\|_p \equiv \mathbb{E}[|X|^p]^{1/p}$ for $p > 1$, which is widely used in statistics. Substituting $r = 1$ and $s = p$ in Eq. (21), we obtain the bound for the p -norm as follows:

$$\frac{\|N(\tau)\|_p}{\|N(\tau)\|_1} \geq \sin \left[\frac{1}{2} \int_0^\tau \frac{\sqrt{\mathcal{B}(t)}}{t} dt \right]^{-\frac{2(p-1)}{p}} \quad (p > 1), \quad (23)$$

which holds for $0 \leq (1/2) \int_0^\tau \sqrt{\mathcal{B}(t)}/t dt \leq \pi/2$. Similarly, Eq. (22) yields

$$\frac{\|N(\tau)\|_p}{\|N(\tau)\|_1} \geq \frac{1}{(1 - e^{-\mathbf{a}(0)\tau})^{\frac{p-1}{p}}}. \quad (24)$$

For $p = 2$, Eqs. (23) and (24) recover the thermodynamic uncertainty relations for the mean and variance of $N(\tau)$:

$$\frac{\text{Var}[|N(\tau)|]}{\mathbb{E}[|N(\tau)|]^2} \geq \tan \left[\frac{1}{2} \int_0^\tau \frac{\sqrt{\mathcal{B}(t)}}{t} dt \right]^{-2}, \quad (25)$$

and

$$\frac{\text{Var}[|N(\tau)|]}{\mathbb{E}[|N(\tau)|]^2} \geq \frac{1}{e^{\mathbf{a}(0)\tau} - 1}, \quad (26)$$

where $\text{Var}[X] \equiv \mathbb{E}[X^2] - \mathbb{E}[X]^2$ denotes the variance of X . The absolute value symbol on the left side of Eqs. (25) and (26) can be removed because $\text{Var}[N(\tau)]/\mathbb{E}[N(\tau)]^2 \geq \text{Var}[|N(\tau)|]/\mathbb{E}[|N(\tau)|]^2$, which follows from $\mathbb{E}[|N(\tau)|] \geq \mathbb{E}[N(\tau)]$ and $\text{Var}[|N(\tau)|] \leq \text{Var}[N(\tau)]$. Note that Eq. (25) was reported in Ref. [40]. Conventionally, the classical thermodynamic uncertainty relation for the dynamical activity is given by [3, 5]

$$\frac{\text{Var}[N(\tau)]}{\mathbb{E}[N(\tau)]^2} \geq \frac{1}{\mathbf{a}_{\text{ss}}\tau}, \quad (27)$$

where $\mathbf{a}_{\text{ss}} \equiv \sum_{\nu, \mu} (\nu \neq \mu) P_{\text{ss}}(\mu) W_{\nu\mu}$ denotes the dynamical activity [Eq. (8)] under steady-state conditions and $P_{\text{ss}}(\mu)$ is the steady-state distribution. While Eq. (27) necessitates the steady-state condition, the condition is not required for Eq. (26). As mentioned above, Eq. (25) is derived from Eq. (23). Although the reverse is not applicable, we can use the Lyapunov inequality to establish a weaker bound for the p -norm using Eq. (25). For the random variable X , the Lyapunov inequality states

$$\|X\|_r \leq \|X\|_s, \quad (28)$$

for $0 < r < s$. Using Eq. (28) and from Eq. (25), we obtain

$$\frac{\|N(\tau)\|_p}{\|N(\tau)\|_1} \geq \sin \left[\frac{1}{2} \int_0^\tau \frac{\sqrt{\mathcal{A}(t)}}{t} dt \right]^{-1} \quad (p > 2). \quad (29)$$

Since $\sin(x)^p \geq \sin(x)^{2(p-1)}$ for $0 \leq x \leq \pi/2$ and $p > 2$, Eq. (29) is weaker than Eq. (23). Moreover, we cannot calculate the bound for $1 < p < 2$ using the Lyapunov inequality, while Eq. (23) holds for $1 < p < 2$.

Discussion

This study derived tradeoff relations using concentration inequalities, typically discussed in terms of information inequalities, such as the Cramér-Rao inequality. Although the tradeoff relations obtained by the information and concentration inequalities differ, they can be understood in the context of a thermodynamic uncertainty relation. The following thermodynamic uncertainty relation is known [40]:

$$\begin{aligned} & \left(\frac{\sqrt{\text{Var}[N(t_2)]} + \sqrt{\text{Var}[N(t_1)]}}{\mathbb{E}[N(t_2)] - \mathbb{E}[N(t_1)]} \right)^2 \\ & \geq \tan \left[\frac{1}{2} \int_{t_1}^{t_2} \frac{\sqrt{\mathcal{B}(t)}}{t} dt \right]^{-2}, \end{aligned} \quad (30)$$

where $0 < t_1 < t_2$. First, let us consider short-time limits, that is, t_1 and t_2 are infinitesimally close. When $t_2 = \tau$ and $t_1 = \tau - \epsilon$, where ϵ is infinitesimally small, Eq. (30) reduces to

$$\frac{\text{Var}[N(\tau)]}{\tau^2 (\partial_\tau \mathbb{E}[N(\tau)])^2} \geq \frac{1}{\mathcal{B}(\tau)}. \quad (31)$$

which can be derived via the Cramér–Rao inequality [17]. The classical case of Eq. (31) was derived in Refs. [3, 5], where the quantum dynamical activity $\mathcal{B}(\tau)$ is replaced by the classical dynamical activity $\mathcal{A}(\tau)$. In contrast, when t_1 and t_2 are far apart, that is, $t_2 = \tau$ and $t_1 = 0$, Eq. (30) agrees with Eq. (25), which was derived from the concentration inequality in this study. From this observation, the short-term case corresponds to information inequality, whereas the long-term case corresponds to concentration inequality. This shows that the Cramér–Rao inequality uses information only around τ whereas the concentration inequality uses information within the range of $[0, \tau]$. This implies that concentration and information inequalities exploit the complementary aspects of Markov processes.

The approach presented in this study lays the foundation for uncovering new uncertainty relations by combining the thermodynamic concentration inequalities with other prevalent ones. In this study, we focused on the probability $P(N(\tau) = 0)$. We can consider, for example, the possibility of examining a probability distribution other than $P(N(\tau) = 0)$. Similarly, we could also take into account thermodynamic costs not restricted to dynamical activity. We reserve these generalisations for future research.

METHODS

Continuous measurement

We review the basics of continuous measurement formalism in open quantum dynamics. Let us define the non-Hermitian effective Hamiltonian:

$$H_{\text{eff}} \equiv H_S - \frac{i}{2} \sum_{m=1}^{N_C} L_m^\dagger L_m. \quad (32)$$

By using Eq. (32), we can express Eq. (3) in the following manner at the $O(dt)$ order:

$$\begin{aligned} \rho_S(t+dt) &= \rho_S(t) - idt \left(H_{\text{eff}} \rho_S(t) - \rho_S(t) H_{\text{eff}}^\dagger \right) \\ &+ dt \sum_{m=1}^{N_C} L_m \rho_S(t) L_m^\dagger. \end{aligned} \quad (33)$$

From Eq. (33), it can be seen that the dynamics are described by the continuous state transitions by the non-Hermitian operator H_{eff} , and the discontinuous state changes by the jump operator L_m . Because a completely

positive and trace-preserving map can be represented using the Kraus representation, the time evolution in Eq. (33) can be described using the Kraus representation:

$$\rho_S(t+dt) = \sum_{m=0}^{N_C} V_m \rho_S(t) V_m^\dagger, \quad (34)$$

where V_m is the Kraus operator defined as

$$V_0 = \mathbb{I}_S - idt H_{\text{eff}}, \quad (35)$$

$$V_m = \sqrt{dt} L_m \quad (1 \leq m \leq N_C). \quad (36)$$

Owing to the completeness relation, V_m should satisfy $\sum_{m=0}^{N_C} V_m^\dagger V_m = \mathbb{I}_S$, where \mathbb{I}_S is the identity operator of the system.

The Kraus representation in Eq. (34) allows identifying the dynamics of the Lindblad equation as a consequence of the measurement, where m denotes the measurement output. Specifically, when the output is m , the post-measurement state becomes $\rho_S(t+dt) = V_m \rho_S(t) V_m^\dagger / \text{Tr}_S[V_m \rho_S(t) V_m^\dagger]$. Suppose that the dynamics starts at $t = 0$ and ends at $t = \tau$. Let J be a sufficiently large integer, and $dt = \tau/J$. Applying Eq. (34) repeatedly, $\rho_S(\tau)$ is represented by

$$\rho_S(\tau) = \sum_{\mathbf{m}} V_{m_{J-1}} \cdots V_{m_0} \rho_S(0) V_{m_0}^\dagger \cdots V_{m_{J-1}}^\dagger, \quad (37)$$

Here, $\mathbf{m} \in \{0, 1, \dots, N_C\}^J$ denotes the measurement record. The variable \mathbf{m} represents whether a jump occurs at each short interval dt . This information can also be expressed by specifying the time t_k at which each jump occurs and the type of jump m_k ($1 \leq m_k \leq N_C$), which is essentially ζ_τ as outlined in Eq. (5).

Bound on the fidelity

We review the upper bound of fidelity in Ref. [40], which is used for the thermodynamic concentration inequalities.

Let $|\psi(t)\rangle$ be a general state vector at time t of general quantum dynamics. Let $\mathcal{J}(t)$ be the quantum Fisher information with respect to t , given by

$$\mathcal{J}(t) \equiv 4 \left[\langle \partial_t \psi(t) | \partial_t \psi(t) \rangle - |\langle \partial_t \psi(t) | \psi(t) \rangle|^2 \right]. \quad (38)$$

Then, the following inequality holds [26, 49]:

$$\frac{1}{2} \int_{t_1}^{t_2} dt \sqrt{\mathcal{J}(t)} \geq \arccos |\langle \psi(t_2) | \psi(t_1) \rangle|, \quad (39)$$

where the left-hand side represents the length of the path traversed through time evolution and the right-hand side represents the distance (i.e., the geodesic distance) between $|\psi(t_1)\rangle$ and $|\psi(t_2)\rangle$.

Next, we introduce the matrix product state formalism in the continuous measurement. From the Kraus representation in Eq. (37), the following continuous matrix product state representation is considered:

$$|\Phi(\tau)\rangle = \sum_{\mathbf{m}} \mathcal{V}_{\mathbf{m}} |\psi_S(0)\rangle \otimes |\mathbf{m}\rangle, \quad (40)$$

where $\mathcal{V}_{\mathbf{m}} \equiv V_{m_{J-1}} \cdots V_{m_0}$, $\mathbf{m} \equiv [m_{J-1}, \dots, m_0]$, and $|\psi_S(0)\rangle$ is the initial state vector ($\rho_S(0) = |\psi_S(0)\rangle \langle \psi_S(0)|$). Considering $dt \rightarrow 0$ limit in Eq. (40), while keeping τ constant, $|\Psi(t)\rangle$ can be represented as a continuous matrix product state [50, 51]:

$$|\Phi(\tau)\rangle = \mathcal{U}(\tau) |\psi_S(0)\rangle \otimes |\text{vac}\rangle, \quad (41)$$

where $\mathcal{U}(t)$ is the operator defined by

$$\mathcal{U}(t) = \mathbb{T} e^{-i \int_0^t dt' (H_{\text{eff}} \otimes \mathbb{I}_F + \sum_m i L_m \otimes \phi_m^\dagger(t'))}. \quad (42)$$

Here, \mathbb{T} denotes the time-ordering operator, \mathbb{I}_F is the identity operator in the field, $\phi_m(t)$ is a field operator that satisfies the canonical commutation relation $[\phi_m(t), \phi_{m'}^\dagger(t')] = \delta_{mm'} \delta(t - t')$, and $|\text{vac}\rangle$ denotes the vacuum state. Within this setting, the continuous matrix product state captures all the continuous measurement information by generating particles by applying $\phi_m^\dagger(t)$ to the vacuum state. The benefit of using the continuous matrix product state for continuous measurements is its ability to embed jump events and the system state into a pure state $|\Phi(t)\rangle$.

The continuous matrix product state given by Eqs. (41) and (42) is inconvenient for evaluating the fidelity between two states at different times t_1 and t_2 , $\langle \Phi(t_2) | \Phi(t_1) \rangle$. This is because evaluating the fidelity between two continuous matrix product states, denoted by $\langle \Phi(t_2) | \Phi(t_1) \rangle$, where $t_1 \neq t_2$ is unfeasible owing to the different integration ranges for $|\Phi(t_1)\rangle$ and $|\Phi(t_2)\rangle$ as shown in Eqs. (41) and (42). Consequently, in our study, we adopt a scaled continuous matrix product state [40]:

$$|\Psi(t)\rangle \equiv \mathcal{V}(\theta) |\psi_S(0)\rangle \otimes |\text{vac}\rangle, \quad (43)$$

where $\theta \equiv t/\tau$ is the scaled time and

$$\mathcal{V}(\theta) \equiv \mathbb{T} e^{\int_0^\tau ds (-i\theta H_{\text{eff}} \otimes \mathbb{I}_F + \sqrt{\theta} \sum_m L_m \otimes \phi_m^\dagger(s))}. \quad (44)$$

Using this representation, we can consider the time evolution of $|\Psi(t)\rangle$ to evaluate the fidelity at different times because the integration range in Eq. (44) does not depend on t .

Consider the geometric relation given by Eq. (39) for the scaled continuous matrix product state $|\Psi(t)\rangle$. Then, we have the following relation [40]:

$$\frac{1}{2} \int_0^\tau \frac{\sqrt{\mathcal{B}(t)}}{t} dt \geq \arccos |\langle \Psi(\tau) | \Psi(0) \rangle|. \quad (45)$$

where $\mathcal{B}(t)$ is defined as

$$\mathcal{B}(t) = 4t^2 \left(\langle \partial_t \Psi(t) | \partial_t \Psi(t) \rangle - |\langle \Psi(t) | \partial_t \Psi(t) \rangle|^2 \right), \quad (46)$$

which is the quantum dynamical activity. Although the right-hand side includes τ , it can be demonstrated that $\mathcal{B}(t)$ does not depend on the choice of τ .

Quantum dynamical activity

Quantum dynamical activity is important in tradeoff relations [17, 40, 42–44]. For example, for the counting observable $N(\tau)$ that counts the number of jump events within $[0, \tau]$ under steady-state conditions, the following quantum thermodynamic uncertainty relation holds [17]:

$$\frac{\text{Var}[N(\tau)]}{\mathbb{E}[N(\tau)]^2} \geq \frac{1}{\mathcal{B}(\tau)}, \quad (47)$$

which was derived via the quantum Cramér-Rao inequality. When we replace $\mathcal{B}(\tau)$ in Eq. (47) with $\mathcal{A}(\tau)$, it becomes identical to the bound reported in Ref. [3]. The exact expression for $\mathcal{B}(t)$ in the quantum dynamical activity defined in Eq. (46) was recently obtained [43]:

$$\mathcal{B}(\tau) = \mathcal{A}(\tau) + \mathcal{C}(\tau), \quad (48)$$

where $\mathcal{A}(\tau)$ denotes the classical dynamical activity [Eq. (9)] and $\mathcal{C}(t)$ is the coherent dynamics contribution given by

$$\begin{aligned} \mathcal{C}(\tau) \equiv & 8 \int_0^\tau ds_1 \int_0^{s_1} ds_2 \text{Re}[\text{Tr}_S \{ H_{\text{eff}}^\dagger \tilde{H}_S(s_1 - s_2) \rho_S(s_2) \}] \\ & - 4 \left(\int_0^\tau ds \text{Tr}_S [H_S \rho_S(s)] \right)^2. \end{aligned} \quad (49)$$

Here, $\tilde{H}_S(t) \equiv e^{\mathcal{L}^\dagger t} H_S$ is interpreted as the Hamiltonian H_S in the Heisenberg picture, where \mathcal{L}^\dagger is the adjoint superoperator

$$\mathcal{L}^\dagger \mathcal{O} \equiv i [H_S, \mathcal{O}] + \sum_{m=1}^{N_C} \mathcal{D}^\dagger [L_m] \mathcal{O}. \quad (50)$$

and \mathcal{D}^\dagger is the adjoint dissipator:

$$\mathcal{D}^\dagger [L] \mathcal{O} \equiv L^\dagger \mathcal{O} L - \frac{1}{2} \{ L^\dagger L, \mathcal{O} \}, \quad (51)$$

Here, \mathcal{O} is an operator. As indicated previously, the classical dynamical activity quantifies the degree of activity of the system and can be evaluated using jump statistics. The quantum dynamical activity also quantifies the system's activity for quantum Markov processes. However, state changes can occur even when there is no jump in the quantum Markov processes owing to the coherent dynamics induced by the Hamiltonian H_S ; $\mathcal{C}(\tau)$ in Eq. (48) reflects such contributions. Apparently, for the classical limit, where $H_S = 0$, $\mathcal{B}(\tau)$ is reduced to $\mathcal{A}(\tau)$. In Ref. [42], an intermediate expression for $\mathcal{B}(t)$ was derived. Under steady-state conditions, the classical dynamical activity $\mathcal{A}(\tau)$ increases linearly as a function of τ , $\mathcal{A}(\tau) = \alpha_{\text{ss}} \tau$. However, the quantum dynamical activity exhibits superlinear scaling within a certain interval, even under steady-state conditions, owing to coherent dynamics [43]. In Ref. [17], an asymptotic expression of $\mathcal{B}(\tau)$ for $\tau \rightarrow \infty$ was derived, revealing that $\mathcal{B}(\tau)$ increases linearly as a function of τ for a sufficiently large τ .

Derivation of the thermodynamic concentration inequality for quantum dynamics

Here, we provide the proofs of Eqs. (10) and (12). From Eq. (40), the probability of no jump $\mathbf{p}(\tau)$ is

$$\mathbf{p}(\tau) = \langle \psi_S(0) | \mathcal{V}_0^\dagger \mathcal{V}_0 | \psi_S(0) \rangle, \quad (52)$$

which satisfies the following inequality:

$$\begin{aligned} |\langle \Psi(0) | \Psi(\tau) \rangle|^2 &= |\langle \psi_S(0) | \mathcal{V}_0 | \psi_S(0) \rangle|^2 \\ &\leq \left| \langle \psi_S(0) | \mathcal{V}_0^\dagger \mathcal{V}_0 | \psi_S(0) \rangle \right| \\ &= \mathbf{p}(\tau). \end{aligned} \quad (53)$$

For the first two lines, we used the Cauchy-Schwarz inequality. Moreover, from Eq. (45), we obtain the following relation for $0 \leq \frac{1}{2} \int_0^\tau \frac{\sqrt{\mathcal{B}(t)}}{t} dt \leq \frac{\pi}{2}$:

$$\cos \left[\frac{1}{2} \int_0^\tau \frac{\sqrt{\mathcal{B}(t)}}{t} dt \right] \leq |\langle \Psi(\tau) | \Psi(0) \rangle|. \quad (54)$$

From Eqs. (53) and (54), we obtain

$$\cos \left[\frac{1}{2} \int_0^\tau \frac{\sqrt{\mathcal{B}(t)}}{t} dt \right]^2 \leq \mathbf{p}(\tau). \quad (55)$$

Next, we associate $\mathbf{p}(\tau)$ with probability $P(N(\tau) = 0)$. When there is no jump within the interval $[0, \tau]$, the observable is $N(\tau) = 0$ due to the condition in Eq. (6); however, the inverse is not necessarily true. Subsequently, the following relation holds:

$$P(N(\tau) = 0) \geq \mathbf{p}(\tau). \quad (56)$$

When the weight vector $[C_\mu]_\mu$ is positive for all the elements, the equality in Eq. (56) holds. Combining Eqs. (55) and (56) completes the proofs of Eqs. (10) and (11).

Derivation of the thermodynamic concentration inequality for classical dynamics

For a classical Markov process with a time-independent transition rate, the probability of no jump $\mathbf{p}(\tau)$ is expressed as

$$\mathbf{p}(\tau) = \sum_\mu P(\mu; 0) e^{-\tau \sum_{\nu(\neq \mu)} W_{\nu\mu}}. \quad (57)$$

Applying the Jensen inequality, we obtain

$$\begin{aligned} \sum_\mu P(\mu; 0) e^{-\tau \sum_{\nu(\neq \mu)} W_{\nu\mu}} &\geq e^{-\tau \sum_\mu P(\mu; 0) \sum_{\nu(\neq \mu)} W_{\nu\mu}} \\ &= e^{-\tau \mathbf{a}(0)}, \end{aligned} \quad (58)$$

which, along with Eq. (56), completes Eq. (12).

Derivation of the observable expectation bound

Let X be a random variable and X_{\max} be its maximum value. Subsequently, substituting these into Eq. (2), the following relation holds for $X_{\max} > a$:

$$P(X \leq a) \leq \frac{\mathbb{E}[X_{\max} - X]}{X_{\max} - a}. \quad (59)$$

Equation (59) is the reverse Markov inequality. Substituting $a = 0$, $X = |N(\tau)|$, and $X_{\max} = N_{\max} \equiv \max |N(\tau)|$ into Eq. (59), we have

$$P(|N(\tau)| \leq 0) \leq 1 - \frac{\mathbb{E}[|N(\tau)|]}{N_{\max}}. \quad (60)$$

Using $P(N(\tau) = 0) = P(|N(\tau)| \leq 0)$ and Eqs. (10) and (12), we obtain Eqs. (13) and (14).

Correlation bound

The bound for the correlation function was obtained in Ref. [45]. The concentration inequalities in Eq. (14) can also be used to derive the bound for the correlation function. We focused on the classical case [Eq. (4)], and let $X(t) \in \mathfrak{B}$ be the state at time t in the classical Markov process. We introduce the score function $S(B_\nu)$ that takes the state $B_\nu (\nu \in \{1, 2, \dots, N\})$ and outputs a real value within $(-\infty, \infty)$. We define $S_{\max} \equiv \max_{B \in \mathcal{B}} |S(B)|$ to represent the highest absolute value of the score function within the set \mathcal{B} . Similarly, we introduce another score function $T(B_\nu)$ and define T_{\max} . Consider the correlation function $C(t) \equiv \langle S(X(0))T(X(t)) \rangle$, where

$$\begin{aligned} \langle S(X(0))T(X(t)) \rangle &= \sum_{\mu, \nu} T(B_\nu) S(B_\mu) P(\mu; 0) P(\nu; t | \mu; 0) \\ &= \mathbf{1} \mathbf{T} e^{\mathbf{W}t} \mathbf{S} \mathbf{P}(0). \end{aligned} \quad (61)$$

Here, $\mathbf{1} \equiv [1, 1, \dots, 1]$ is the trace state and $\mathbf{S} \equiv \text{diag}[S(B_1), \dots, S(B_N)]$ and $\mathbf{T} \equiv \text{diag}[T(B_1), \dots, T(B_N)]$. For example, consider a classical system with two states $\mathcal{B} = \{B_1, B_2\}$, where $X(t)$ represents random switching between B_1 and B_2 . Here, the score function is typically $S(B_1) = -1$ and $S(B_2) = 1$. The change in the correlation function given by $C(\tau) - C(0)$ can be expressed as $N(\tau)$, as follows:

$$N(\tau) = S(X(0))T(X(\tau)) - S(X(0))T(X(0)). \quad (62)$$

$N(\tau)$ satisfies the condition in Eq. (6) and its expectation provides $\mathbb{E}[N(\tau)] = C(\tau) - C(0)$, which is the change in the correlation function. Substituting Eq. (62) into Eq. (14), we derive the upper bound for the change in the correlation function as follows:

$$|C(0) - C(\tau)| \leq 2S_{\max}T_{\max} \left(1 - e^{-\mathbf{a}(0)\tau} \right). \quad (63)$$

Linear response bound

Here, we derive the bound for a weak perturbation applied to the system [cf. Eq. (74)], based on Ref. [45]. The steady-state probability distribution satisfies

$$\mathbf{W}\mathbf{P}_{\text{ss}} = 0, \quad (64)$$

where $\mathbf{P}_{\text{ss}} \equiv [P_{\text{ss}}(1), \dots, P_{\text{ss}}(M)]^\top$. Suppose a weak perturbation is applied to the master equation of Eq. (4), which corresponds to the following replacement in Eq. (4):

$$\mathbf{W} \rightarrow \mathbf{W} + \chi \mathbf{F} h(t), \quad (65)$$

where $\chi > 0$ is the perturbation strength, \mathbf{F} is an $M \times M$ real matrix, and $h(t)$ is a real function of t . Assuming that χ is sufficiently weak, we employ the perturbation expansion:

$$\mathbf{P}(t) = \mathbf{P}_{\text{ss}} + \chi \mathbf{P}_1(t) + O(\chi^2), \quad (66)$$

where $\mathbf{P}_1(t)$ is a first-order term. Substituting Eqs. (65) and (66) into Eq. (4) and retaining the terms up to the first order in χ , we obtain the following differential equation with respect to $\mathbf{P}_1(t)$:

$$\frac{d}{dt} \mathbf{P}_1(t) = \mathbf{W} \mathbf{P}_1(t) + \mathbf{F} \mathbf{P}_{\text{ss}} h(t). \quad (67)$$

Solving Eq. (67), the solution is

$$\mathbf{P}_1(t) = \int_{-\infty}^t e^{\mathbf{W}(t-t')} \mathbf{F} \mathbf{P}_{\text{ss}} h(t') dt'. \quad (68)$$

Consider the expectation of the score function $G(B)$ for $B \in \mathfrak{B}$, and consider its deviation from the steady-state condition under perturbation:

$$\begin{aligned} \Delta G(t) &\equiv \sum_{\mu} P(\mu; t) G(B_{\mu}) - \sum_{\mu} P_{\text{ss}}(\mu) G(B_{\mu}) \\ &= \chi \int_{-\infty}^{\infty} R_G(t-t') h(t') dt', \end{aligned} \quad (69)$$

where $R_G(t)$ is the linear response function given by

$$R_G(t) = \begin{cases} \mathbf{1} \mathbf{G} e^{\mathbf{W}t} \mathbf{F} \mathbf{P}_{\text{ss}} & t \geq 0, \\ 0 & t < 0. \end{cases} \quad (70)$$

Knowing the linear response function $R_G(t)$, we can evaluate any input-output relation in the linear response regime. Next, we associate the linear response function with the correlation function. Using matrix notation, the correlation function can be expressed by [45]

$$C(t) = \mathbf{1} \mathbf{T} e^{\mathbf{W}t} \mathbf{S} \mathbf{P}_{\text{ss}}. \quad (71)$$

From Eq. (71), the time derivative of $C(t)$ is

$$\frac{d}{dt} C(t) = \mathbf{1} \mathbf{T} e^{\mathbf{W}t} \mathbf{W} \mathbf{S} \mathbf{P}_{\text{ss}}. \quad (72)$$

Comparing Eq. (70) with Eq. (72), when the system satisfies $\mathbf{G} = \mathbf{T}$ and $\mathbf{F} = \mathbf{W} \mathbf{S}$, then the linear response function $R_T(t)$ is given by $\partial_t C(t)$. Suppose a constant perturbation is initiated at $t = 0$. This perturbation can be modelled as $h(t) = \Theta(t)$, where $\Theta(t)$ denotes the Heaviside step function. Therefore, ΔT can be expressed as

$$\begin{aligned} \Delta T(t) &= \chi \int_{-\infty}^{\infty} R_T(t-t') \Theta(t') dt' \\ &= \chi \int_0^t R_T(t-t') dt' \\ &= \chi (C(t) - C(0)). \end{aligned} \quad (73)$$

Using Eqs. (63) and (73), we obtain

$$|\Delta T(\tau)| \leq 2\chi S_{\text{max}} T_{\text{max}} (1 - e^{-\mathbf{a}_{\text{ss}} \tau}), \quad (74)$$

where \mathbf{a}_{ss} is the dynamical activity under steady-state conditions.

ACKNOWLEDGEMENTS

This work was supported by JSPS KAKENHI Grant Number JP23K24915.

AUTHOR CONTRIBUTIONS

Y.H. contributed to the conceptualisation, performed analytical calculations, and drafted the manuscript. T.N. performed analytical calculations.

COMPETING INTERESTS

The authors declare no conflict of interest.

[1] A. C. Barato and U. Seifert, Thermodynamic uncertainty relation for biomolecular processes, *Phys. Rev. Lett.* **114**, 158101 (2015).

[2] T. R. Gingrich, J. M. Horowitz, N. Perunov, and J. L. England, Dissipation bounds all steady-state current fluctuations, *Phys. Rev. Lett.* **116**, 120601 (2016).

- [3] J. P. Garrahan, Simple bounds on fluctuations and uncertainty relations for first-passage times of counting observables, *Phys. Rev. E* **95**, 032134 (2017).
- [4] A. Dechant and S.-i. Sasa, Current fluctuations and transport efficiency for general Langevin systems, *J. Stat. Mech: Theory Exp.* **2018**, 063209 (2018).
- [5] I. Di Terlizzi and M. Baiesi, Kinetic uncertainty relation, *J. Phys. A: Math. Theor.* **52**, 02LT03 (2019).
- [6] Y. Hasegawa and T. Van Vu, Uncertainty relations in stochastic processes: An information inequality approach, *Phys. Rev. E* **99**, 062126 (2019).
- [7] Y. Hasegawa and T. Van Vu, Fluctuation theorem uncertainty relation, *Phys. Rev. Lett.* **123**, 110602 (2019).
- [8] A. Dechant and S.-i. Sasa, Fluctuation–response inequality out of equilibrium, *Proc. Natl. Acad. Sci. U.S.A.* **117**, 6430 (2020).
- [9] V. T. Vo, T. Van Vu, and Y. Hasegawa, Unified approach to classical speed limit and thermodynamic uncertainty relation, *Phys. Rev. E* **102**, 062132 (2020).
- [10] T. Koyuk and U. Seifert, Thermodynamic uncertainty relation for time-dependent driving, *Phys. Rev. Lett.* **125**, 260604 (2020).
- [11] P. Erker, M. T. Mitchison, R. Silva, M. P. Woods, N. Brunner, and M. Huber, Autonomous quantum clocks: Does thermodynamics limit our ability to measure time?, *Phys. Rev. X* **7**, 031022 (2017).
- [12] K. Brandner, T. Hanazato, and K. Saito, Thermodynamic bounds on precision in ballistic multiterminal transport, *Phys. Rev. Lett.* **120**, 090601 (2018).
- [13] F. Carollo, R. L. Jack, and J. P. Garrahan, Unraveling the large deviation statistics of Markovian open quantum systems, *Phys. Rev. Lett.* **122**, 130605 (2019).
- [14] J. Liu and D. Segal, Thermodynamic uncertainty relation in quantum thermoelectric junctions, *Phys. Rev. E* **99**, 062141 (2019).
- [15] G. Guarnieri, G. T. Landi, S. R. Clark, and J. Goold, Thermodynamics of precision in quantum nonequilibrium steady states, *Phys. Rev. Research* **1**, 033021 (2019).
- [16] S. Saryal, H. M. Friedman, D. Segal, and B. K. Agarwalla, Thermodynamic uncertainty relation in thermal transport, *Phys. Rev. E* **100**, 042101 (2019).
- [17] Y. Hasegawa, Quantum thermodynamic uncertainty relation for continuous measurement, *Phys. Rev. Lett.* **125**, 050601 (2020).
- [18] Y. Hasegawa, Thermodynamic uncertainty relation for general open quantum systems, *Phys. Rev. Lett.* **126**, 010602 (2021).
- [19] M. F. Sacchi, Thermodynamic uncertainty relations for bosonic Otto engines, *Phys. Rev. E* **103**, 012111 (2021).
- [20] A. A. S. Kalaei, A. Wacker, and P. P. Potts, Violating the thermodynamic uncertainty relation in the three-level maser, *Phys. Rev. E* **104**, L012103 (2021).
- [21] T. Van Vu and K. Saito, Thermodynamics of precision in Markovian open quantum dynamics, *Phys. Rev. Lett.* **128**, 140602 (2022).
- [22] J. M. Horowitz and T. R. Gingrich, Thermodynamic uncertainty relations constrain non-equilibrium fluctuations, *Nat. Phys.* (2019).
- [23] L. Mandelstam and I. Tamm, The uncertainty relation between energy and time in non-relativistic quantum mechanics, *J. Phys. USSR* **9**, 249 (1945).
- [24] N. Margolus and L. B. Levitin, The maximum speed of dynamical evolution, *Physica D: Nonlinear Phenomena* **120**, 188 (1998).
- [25] S. Deffner and E. Lutz, Generalized Clausius inequality for nonequilibrium quantum processes, *Phys. Rev. Lett.* **105**, 170402 (2010).
- [26] M. M. Taddei, B. M. Escher, L. Davidovich, and R. L. de Matos Filho, Quantum speed limit for physical processes, *Phys. Rev. Lett.* **110**, 050402 (2013).
- [27] A. del Campo, I. L. Egusquiza, M. B. Plenio, and S. F. Huelga, Quantum speed limits in open system dynamics, *Phys. Rev. Lett.* **110**, 050403 (2013).
- [28] S. Deffner and E. Lutz, Energy-time uncertainty relation for driven quantum systems, *J. Phys. A: Math. Theor.* **46**, 335302 (2013).
- [29] D. P. Pires, M. Cianciaruso, L. C. Céleri, G. Adesso, and D. O. Soares-Pinto, Generalized geometric quantum speed limits, *Phys. Rev. X* **6**, 021031 (2016).
- [30] E. O'Connor, G. Guarnieri, and S. Campbell, Action quantum speed limits, *Phys. Rev. A* **103**, 022210 (2021).
- [31] N. Shiraishi, K. Funo, and K. Saito, Speed limit for classical stochastic processes, *Phys. Rev. Lett.* **121**, 070601 (2018).
- [32] S. Ito, Stochastic thermodynamic interpretation of information geometry, *Phys. Rev. Lett.* **121**, 030605 (2018).
- [33] S. Ito and A. Dechant, Stochastic time evolution, information geometry, and the Cramér-Rao bound, *Phys. Rev. X* **10**, 021056 (2020).
- [34] T. Van Vu and Y. Hasegawa, Geometrical bounds of the irreversibility in Markovian systems, *Phys. Rev. Lett.* **126**, 010601 (2021).
- [35] S. Deffner and S. Campbell, Quantum speed limits: from Heisenberg’s uncertainty principle to optimal quantum control, *J. Phys. A: Math. Theor.* **50**, 453001 (2017).
- [36] A. Dechant, Multidimensional thermodynamic uncertainty relations, *J. Phys. A: Math. Theor.* **52**, 035001 (2019).
- [37] F. Fröwis, Kind of entanglement that speeds up quantum evolution, *Phys. Rev. A* **85**, 052127 (2012).
- [38] S. Boucheron, G. Lugosi, and P. Massart, *Concentration Inequalities: A Nonasymptotic Theory of Independence* (Oxford University Press, 2013).
- [39] H. Zhang and S. Chen, Concentration inequalities for statistical inference, *Communications in Mathematical Research* **37**, 1 (2021).
- [40] Y. Hasegawa, Unifying speed limit, thermodynamic uncertainty relation and Heisenberg principle via bulk-boundary correspondence, *Nat. Commun.* **14**, 2828 (2023).
- [41] G. Biroli and J. P. Garrahan, Perspective: The glass transition, *J. Chem. Phys.* **138**, 12A301 (2013).
- [42] S. Nakajima and Y. Utsumi, Symmetric-logarithmic-derivative Fisher information for kinetic uncertainty relations, *Phys. Rev. E* **108**, 054136 (2023).
- [43] T. Nishiyama and Y. Hasegawa, Exact solution to quantum dynamical activity, *Phys. Rev. E* **109**, 044114 (2024).
- [44] T. Nishiyama and Y. Hasegawa, Trade-off relations in open quantum dynamics via Robertson and Maccone-Pati uncertainty relations, *arXiv:2402.09680* (2024).
- [45] Y. Hasegawa, Thermodynamic correlation inequality, *Phys. Rev. Lett.* **132**, 087102 (2024).
- [46] E. Kwon, J.-M. Park, J. S. Lee, and Y. Baek, Unified hierarchical relationship between thermodynamic tradeoff relations, *arXiv:2311.01098* (2023).

- [47] V. V. Petrov, On lower bounds for tail probabilities, *J. Stat. Plann. Inference* **137**, 2703 (2007).
- [48] R. E. A. C. Paley and A. Zygmund, On some series of functions, (3), *Math. Proc. Cambridge Philos. Soc.* **28**, 190-205 (1932).
- [49] A. Uhlmann, The metric of Bures and the geometric phase, in *Groups and Related Topics: Proceedings of the First Max Born Symposium*, edited by R. Gielerak, J. Lukierski, and Z. Popowicz (Springer Netherlands, Dordrecht, 1992) pp. 267–274.
- [50] F. Verstraete and J. I. Cirac, Continuous matrix product states for quantum fields, *Phys. Rev. Lett.* **104**, 190405 (2010).
- [51] T. J. Osborne, J. Eisert, and F. Verstraete, Holographic quantum states, *Phys. Rev. Lett.* **105**, 260401 (2010).